An Investigation of the Properties of Zn Coated Mild Steel

O.S.I Fayomi[*] and A.P.I Popoola[*]

Department of Chemical and Metallurgical Engineering, Tshwane University of Technology, Private Bag X680, Pretoria 0001, South Africa.
[*]E-mail: popoolaapi@tut.ac.za, sunnyfayomi@yahoo.com

Researches in the area of zinc coatings on steel are rather unending because of the unique properties and the very low cost that it offers. In this paper, the mechanical (wear and hardness) and corrosion behaviours of Zn Coated Mild Steel in 3.65% NaCl are described. A thin film of Zn on steel substrates was prepared by electrodeposition technique using Zn particles to form a bath plating solution. Scanning electron microscope and Atomic force microscope were used to study the surface morphology, the topography and the surface adherent properties of the coatings. The crystal particles present were observed by X-ray diffraction pattern (XRD) and energy dispersive X-ray diffraction spectrometer (EDS). The microhardness of deposited plate, the electrochemical behavior and the corrosion properties of the deposits were investigated by means of Vickers microhardness and polarization measurements. The uniform deposits of Zn showed fine grains and good protection against corrosion as appreciated 75% hardness value was achieved.

1. INTRODUCTION

The most widely used material for both domestic and industrial applications owing to its excellent properties remains steel. One of the foremost weaknesses of steel is its corrosion and wear behaviours (1-15). Due to these disadvantages, many protection methods have been adopted to inprove the service life of steel against corrosion and wear attacks (5-12). Among these, electroplating method with metallic thin films of various interests has been worked upon. The interest in zinc electrodeposited coatings for the protection of mild steel is enormous in the engineering industries (1-20). The stability of these coatings and their surface behaviour establishes further development of these coatings for environmental applications. Zinc is widely used as metallic coatings applied to steel surfaces to protect them from corrosion which can be obtained either by hot dipping or electroplating process (10-15). Electrolytic deposition of Zn produce thinner coating as compared to hot dipping method, that is suitable for the subsequent forming process in the automotive industries (4-12).

However, with the choice of proper plating parameters, electrodeposition can still give better coatings with fine surface finish that will exhibit high degree of corrosion resistance and mechanical properties such as micro-hardness, wear resistance, ductility, strength, decorative properties and etc (5-10). The deposited Zn is always richer on the substrate when electrodeposited from the solution containing Zn^{2+}. Many studies have been carried out to understand the characteristics of the deposition process of Zn (12-21). It is found that the characteristics of the deposited coating depend on the applied voltage, current density, pH, bath composition, additives and temperature (10-21). The phases and microstructure of the surface of the deposited Zn is another important characteristic which controls the corrosion resistance and other mechanical properties (15-21). Corrosion properties is however, very sensitive to surface inhomogeneities and segregation of deposition element. The present investigation is to develop the plating bath of suitable composition with zinc powder, study the morphology of coatings surfaces deposited at different voltages. Examination of the electrochemical behaviour of deposited substrate in chloride medium and the establishment of the optimum electrodeposition conditions for good quality Zn coating on mild steel. The mechanical properties of the coatings will also be studied.

2. EXPERIMENTAL METHOD

The electrodeposition of Zn was performed in an electroplating cell of two electrodes where commercial mild steel (40 mm x 20 mm x 1 mm) sheet was used as substrate and zinc sheets (30 mm x 20 mm x 1 mm) was used as anode. Before electroplating commences, mild steel was polished with successive finer grades of emery paper, P60, P120, P320, P400, P6600 grits and finally on the emery cloth then cleaned with Na_2CO_3 solution, descaled by acid pickling operation in 20% 0.5M HCl and activated by dipping in 10% HCl solution at room temperature for 15 seconds followed by rinsing in distilled water. Cathode and Anode were connected to the D.C. power supply through a rectifier. Chemical reagents used are zinc sulphate, zinc chloride, boric acid, leveler and brightener. Deposition was carried out at varying applied voltage of 0.6-1.0 V, 2 A/dm^2 with the bath pH of 4. All the depositions were made at constant time period of 20 minutes. The pH range required for the best deposition was determined from the physical morphology and appearance of the deposited coatings at different applied voltage. Surface structure of the Zn coatings was investigated using Scanning Electron Microscope (SEM). The corrosion resistance of the deposited Zn coatings was investigated in 3.65% NaCl using potentiodynamic polarization.

3. RESULTS AND DISCUSSION

3.1. Characterization of Starting Materials

Chemical composition of mild steel substrate can be seen in Table 1. The SEM spectrum in Figure 2 shows the morphology of mild steel. EDS analysis established the essential elemental composition with Fe being the major constituent.

Table 1. Chemical composition of as-received mild steel

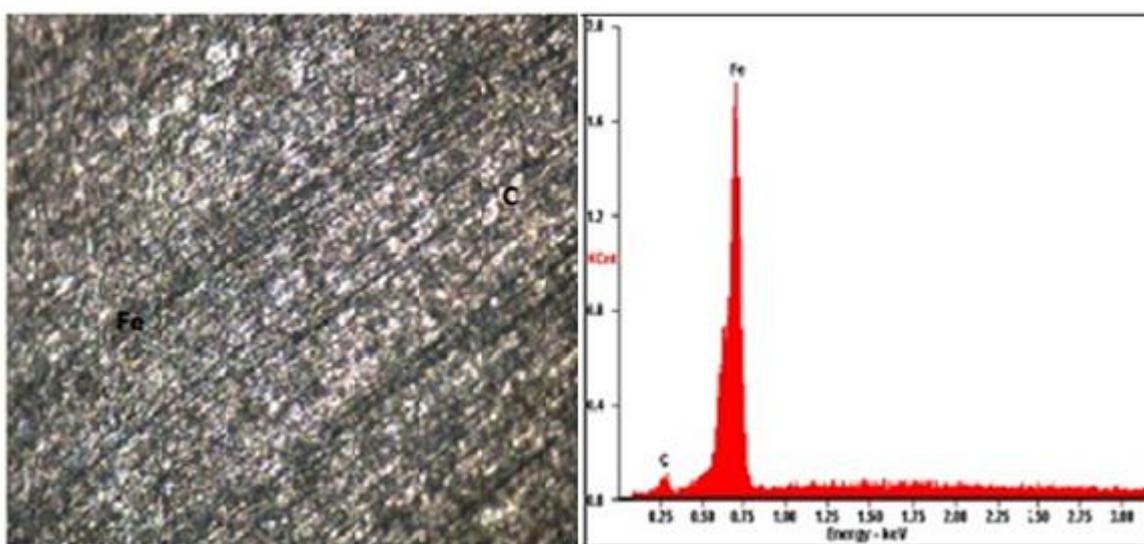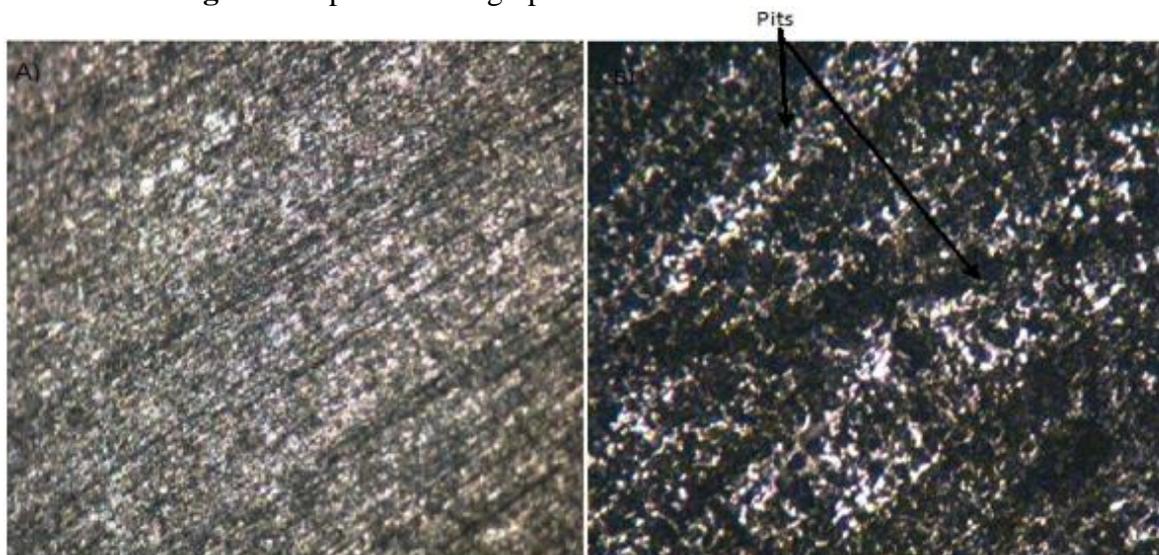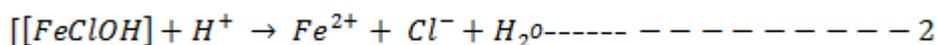| Elements	Composition (wt%)
Carbon	0.150
Silicon	0.180
Manganese	0.450
Sulphur	0.031
Phosphorus	0.010
Nickel	0.008
Aluminum	0.005
Iron	99.166

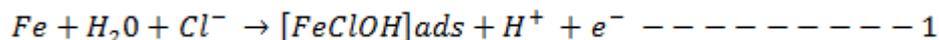**Figure 1.** Optical Micrograph and EDS of as-received mild steel

Figure 2. Optical micrographs of mild steel substrate (a) before and (b) after corrosion test.

From Figure 2, it is evident that the surface lattices become more pronounced with the presence of chloride ions revealing mild steel dissolution.

This mechanism involve electron discharge and the active dissolution of mild steel in sodium chloride solution give an impression that the native oxide film is unstable under the prevailing chloride environment as show in equation 1 and 2 which is in agreement with the suggested mechanism for iron dissolution in chloride environment [22].

$$Fe + H_2O + Cl^- \rightarrow [FeClOH]ads + H^+ + e^- \; ---------1$$

$$[[FeClOH] + H^+ \rightarrow Fe^{2+} + Cl^- + H_2O ------ \; ---------2$$

From all indications, the severe attack of the metal by aggressive chloride anions occurs locally and uniformly. The rough surface observed was basically due to rapid corrosion reactions between the mild steel and chloride anions which almost covers the mild steel surface, revealing pits and uniform corrosion attack occurs [1, 16, and 22]. There are a large number of pits surrounded by iron oxide layer revealing that pit formation under these conditions occurs continuously during the exposure period while iron oxide builds up over the surface.

The electrodeposition processing parameters and results obtained for this study are seen in Table 2. The deposition time and voltage was varied to achieve the results below. It could be seen that the resulting zinc plating thickness varied linearly with plating time. This significant increase in coating thickness and weight gain is a function of applied voltage and corresponding time of deposition which may typically influence the surface properties [10, 12 and 20].

Table 2. Summarized data of plated samples for constant plating time at various voltages.

Sample No	Deposition Time (min)	Deposition Voltage (V)	Plating Effects
Zn 1	20	0.6	Diffused reflection
Zn 2	20	0.8	Fairly bright reflection
Zn 3	20	1.0	Bright reflection
Zn (As-received)	20	-	-

The tendency of electrodeposited surfaces to adhere and thus form materials with fine texture is influenced by the nature of the additive and the purity of the base particles [12, 13 and 14]. Figure 3 shows a SEM micrograph and EDS of the Zn particles which were used for the bath formation. The morphologies of the Zn particles were irregular in shape and size and somehow homogeneous in

distribution, therefore the particles possess a strong bond during electroplating. The powder purity was determined by EDS. The peak shown was that of Zn particle. This shows that the powder used was pure and free from contamination.
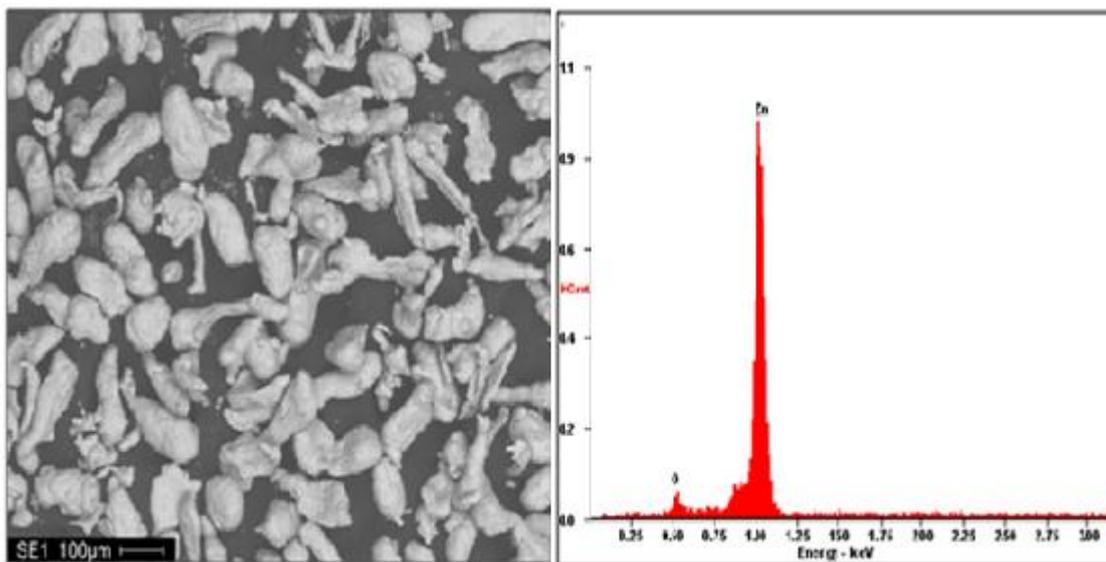

Figure 3. SEM/EDS spectra Zn

3.2. Characterization of Deposits

3.2.1. Atomic Force Microscope Analysis

Figures 4, 5 and 6 show the atomic force micrographs of the deposited samples. Metallographic studies revealed the topography of the deposited zinc on the surface of the substrate. Grain size and crystal growth uniformity was obtained from sample 1 (Figure 4) however, an improvement in crystal growth and uniform arrangement of the crystals was observed in sample 2 (Figure 5) and sample 3 (Figure 6) than the former. This is attributed to the diffusion of electrodepositing ions into the nucleus, meaning that the adsorbed atom wanders to a growth point on the cathode and is incorporated in the growing lattice under the influence of the applied voltage and increased electrodeposition time.

Figure 4 is less rich in zinc deposit, from this micrograph, it can be seen that the coated layer is of less homogeneous distribution. However, a better homogeneous distribution of zinc on the substrate which is crack free and with fewer pores was achieved as a result of the longer deposition time as seen in Figure 6. The distribution of the zinc particles on the substrate is influenced by throwing power, time of immersion and voltage. According to [14] the grain size increases with the film thickness. However in Figure 5 and 6 essential absorption peaks cut across surfaces of deposited sample with significant adhesion, revealing creation of good metallurgical bonds and increased grain size between plating particles and the substrate.

3.2.2. XRD Analysis

Phase examination of the surface layers of the zinc coatings were evaluated through X-ray diffraction. XRD profiles for the Zn 1 and Zn 2 are shown in Figure 7 and 8 respectively. The XRD spectra of these samples shows similar phases but with more diffraction peaks indicated in Figure 9 along the surface of the substrate. Figure 9 shows the XRD spectra for Zn 3 with ZnO_2 and ZnO as predominant crystals within the deposited system and suggesting an adherent metallic coating.

Figure 4. AFM images of the Zn film obtained for sample 1; (a) 2-D image, (b) 3-D relief image and (c) roughness analysis

Figure 5. AFM images of the Zn film obtained for sample 2; (a) 2-D image, (b) 3-D relief image and (c) roughness analysis
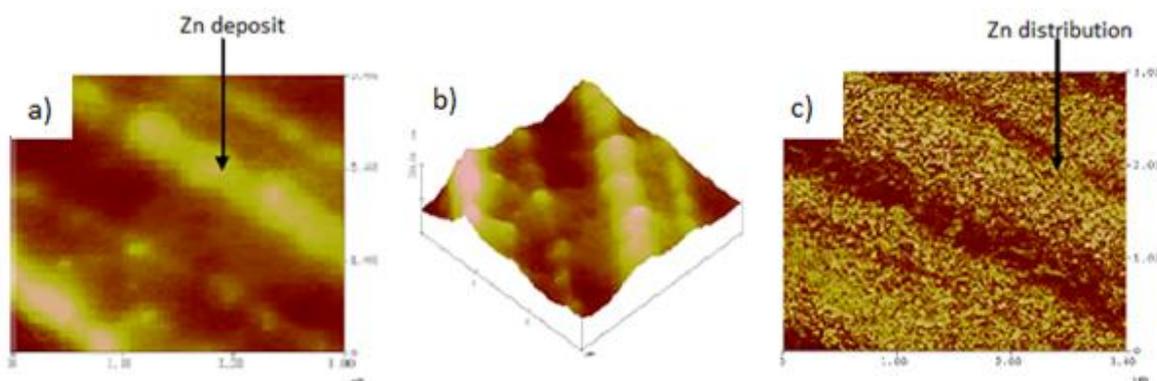

Figure 6. AFM images of the Zn film obtained for sample 3; (a) 2-D image, (b) 3-D relief image and (c) roughness analysis.
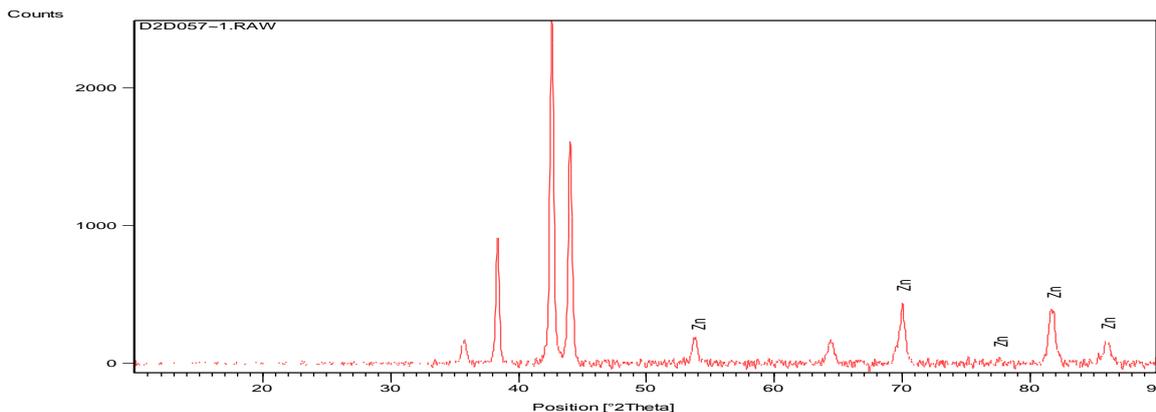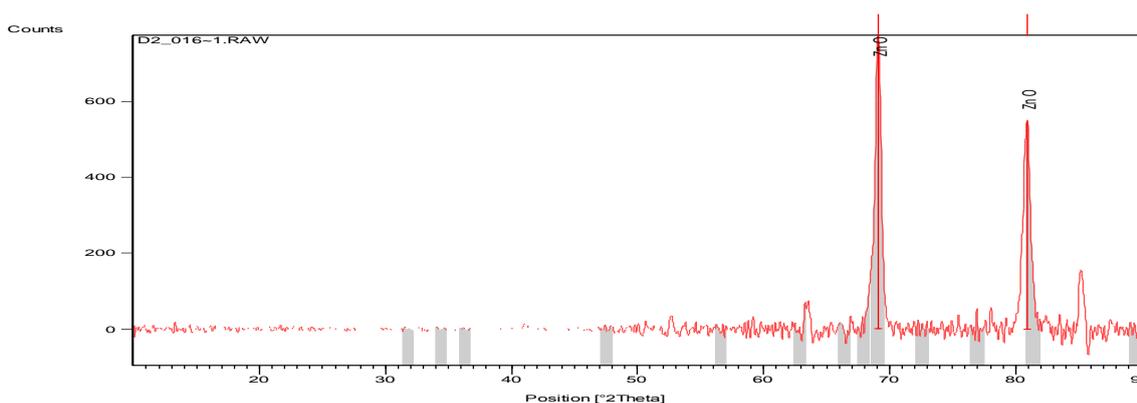
Figure 7. Solid X-ray diffraction profile for Zn 1

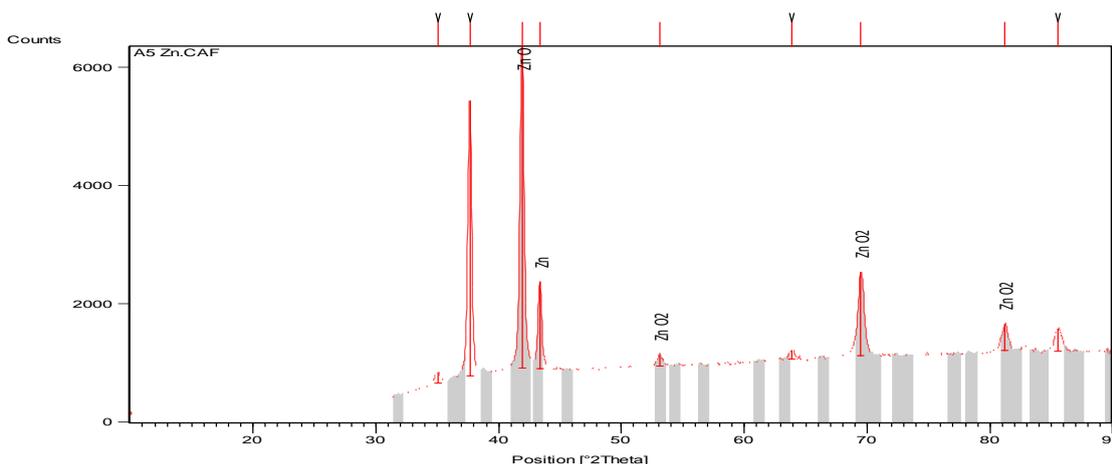**Figure 8.** Solid X-ray diffraction profile for Zn 2

Figure 9. Solid X-ray diffraction profile for Zn 3

3.2.3. SEM/EDS analysis

Figures 10 - 12 illustrates the surface features of the Zn coated samples plated at different voltages. Comparing these micrographs, it can be observed that the Zn films completely covered the substrate. The nature of crystal growth as shown in Figure 10 indicates a coarse–grained deposit having non uniform crystal size.
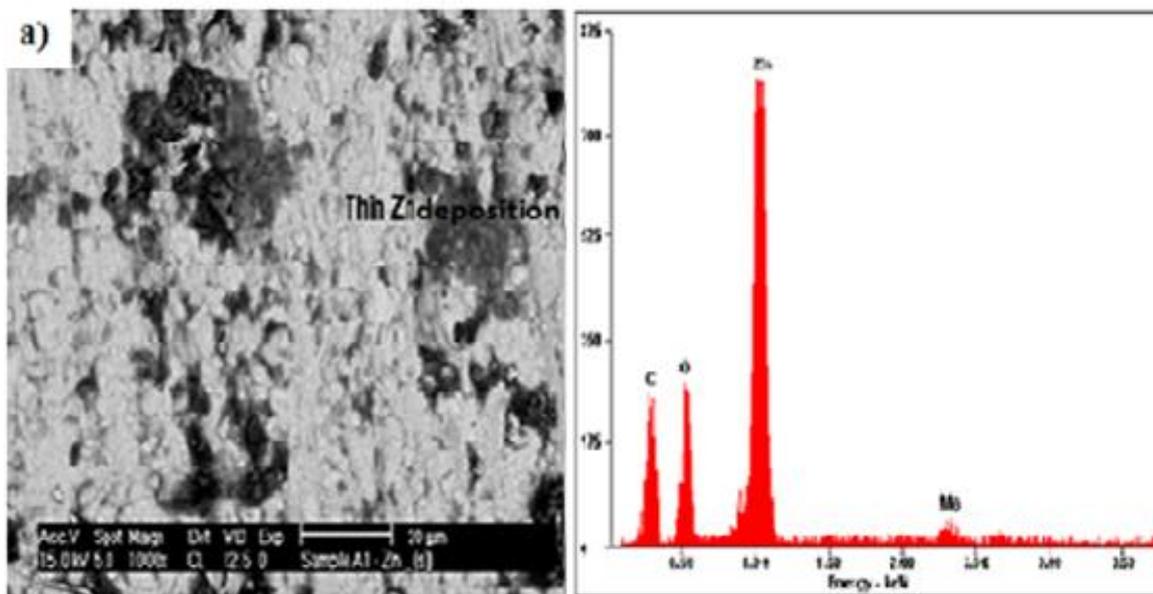
Figure 10. SEM/EDS of Zn 1 showing the surface morphology of the deposited sample

According to [13, 14 and 15] deposit composition can be influence by bath control parameter. Increase in applied potential, regulates the uniform arrangement of crystals and hence results in the fine grained deposits exhibiting coalesced crystallites as showed in Figures 11 and 12 which is in agreement with [14] that the characterization of the deposited coating depend on the applied voltage. EDS analyses performed on the samples revealed that the deposit contains zinc and iron.
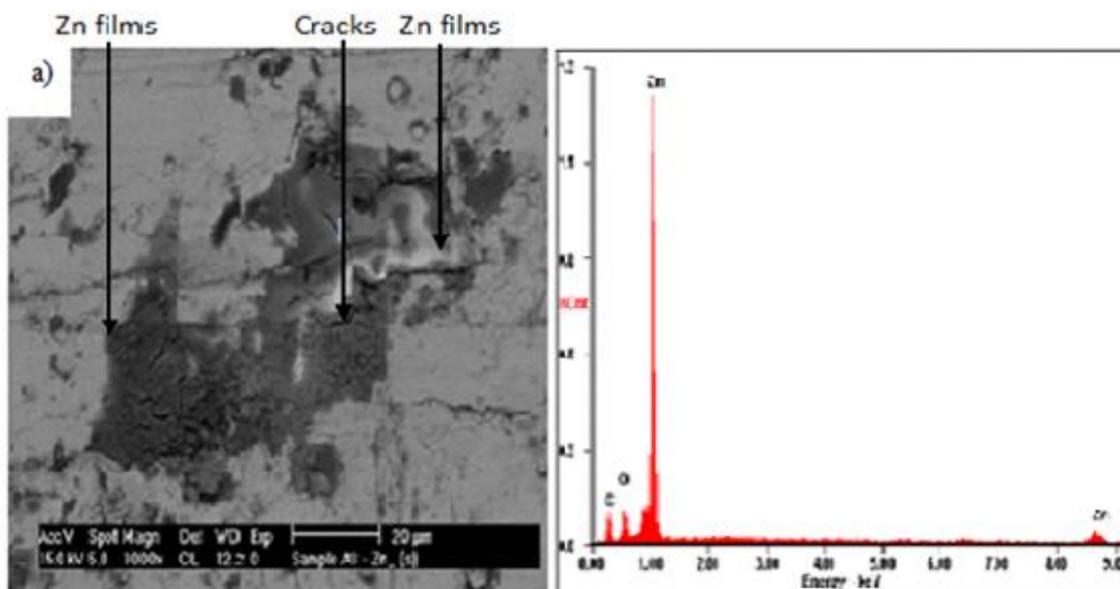

Figure 11. SEM/EDS of Zn 2 showing the surface morphology of the deposited sample.
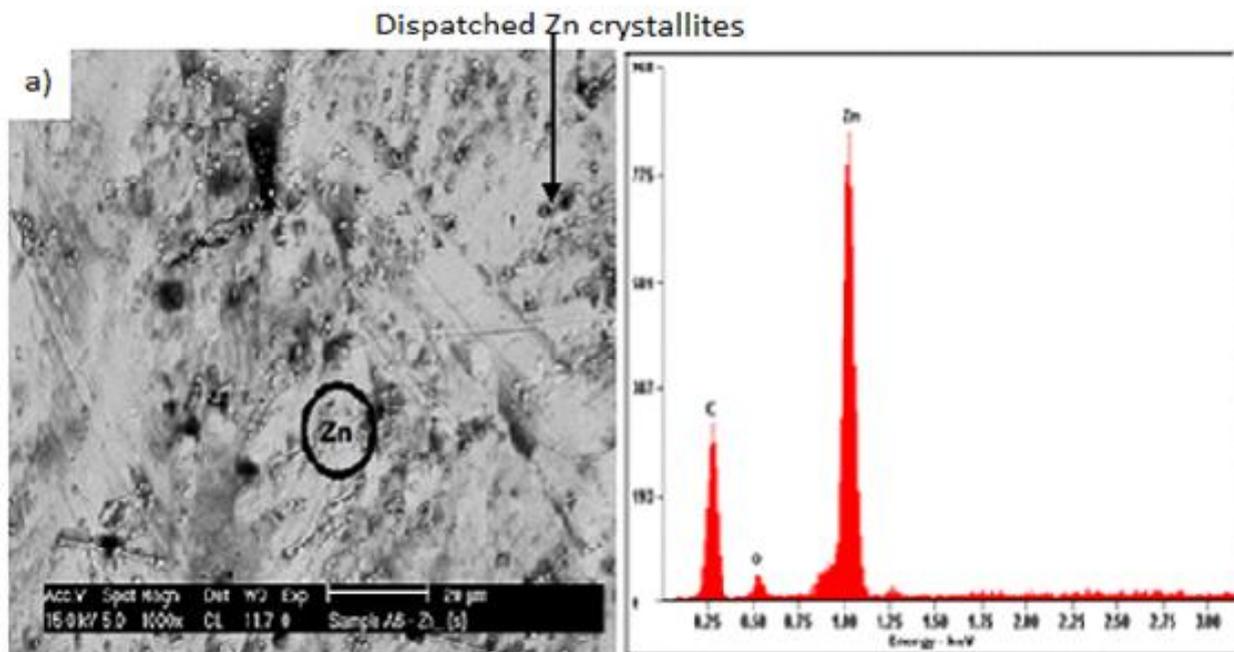
Figure 12. SEM/EDS of Zn 3 showing the surface morphology of the deposited sample

3.2.4. Microhardness Analysis

Electro-deposition of mild steel with zinc resulted in hardness increase from 60 HVN for base mild steel to approximately 85 HVN (cross-section) for the deposited surface of Zn 1 (see Figure 13). The hardness profile data for all the samples shows significant average increase. The average microhardness values for all the samples were calculated, Zn 3 has the highest value of hardness with 108 HVN, (see Figure 13) this is due to the depth of Zn deposited on the sample.
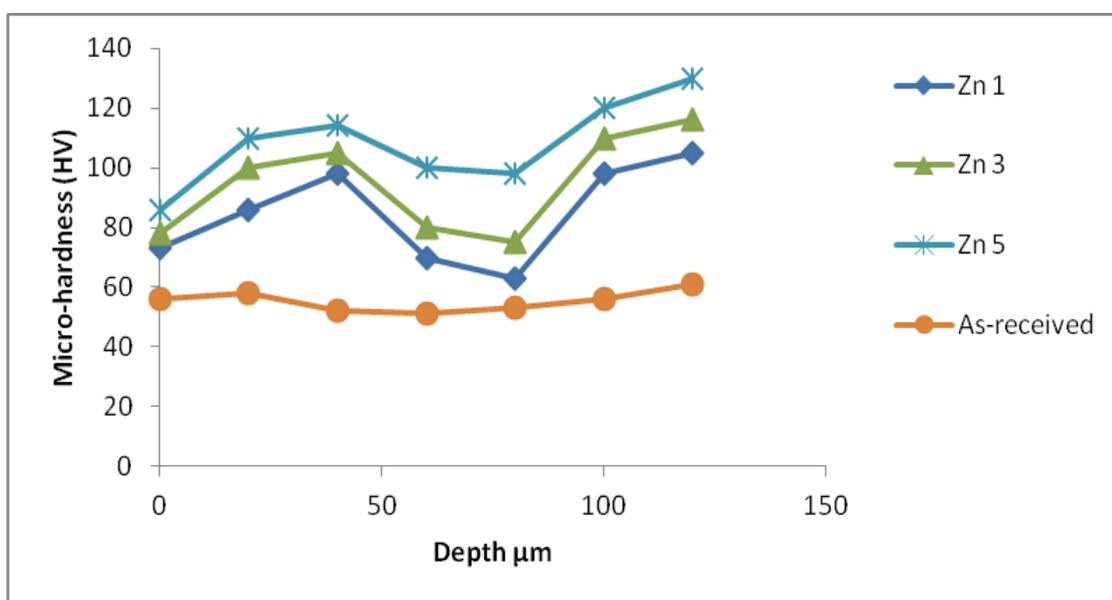

Figure 13. The microhardness/depth profile for zinc deposited sample

This improvement in hardness was attributed to the formation of adhesive properties on the substrate. The microhardness of the Zn deposited samples under different conditions were carefully observed and studied. Experimental results showed that the microhardness property of the zinc deposited sample depend on the operating current density. Previous work by [17], had affirmed that the microstructure evolved in coating depends on the processing parameters and hence such metallurgical parameter influence the grain size which is paramount to the buildup of surface hardness. It was clearly observed that three regions are distinguished on the curve: a region of initial deposit, a middle region and a region of high current density. The microhardness value for the substrate material is 60 HVN. For Zn 1 sample is 85 HVN, for Zn 2 sample is 95 HVN and Zn 3 is 108 HVN. The microhardness of the Zn deposited samples clearly increases with increases in electrodeposition time.

3.3. Wear Rate Evaluation

The graph of the variation of the wear rate as a function of time after deposition (for as-received mild steel and Zn deposited samples) can be seen in Figures 14. Comparisons of the experimental results show that wear resistance increased. The rate of wear is very high for the as-received sample; on other hand, the rate of wear is very low for the Zn 1 and Zn 2 samples. However, Zn 3 displayed a higher wear resistance compared to other deposited sample. The wear rate of as-received sample shows poor wear resistance which is expected.

The wear scar morphology of the Zn deposited steels were used to establish the stability of the coatings on the substrate. Figures 16, 17 and 18 shows the worn surfaces observed after selected wear time on Zn samples. It can be seen from the scars, that severe degree of plastic deformation, massive grooves, and pits dominated the surface of the as received substrate which was really expected (see Figure 15).
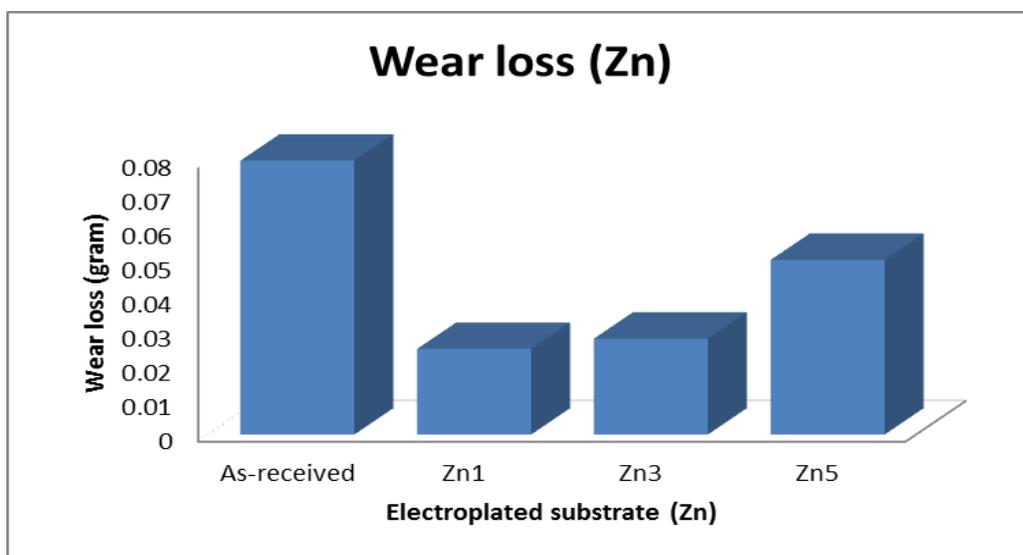

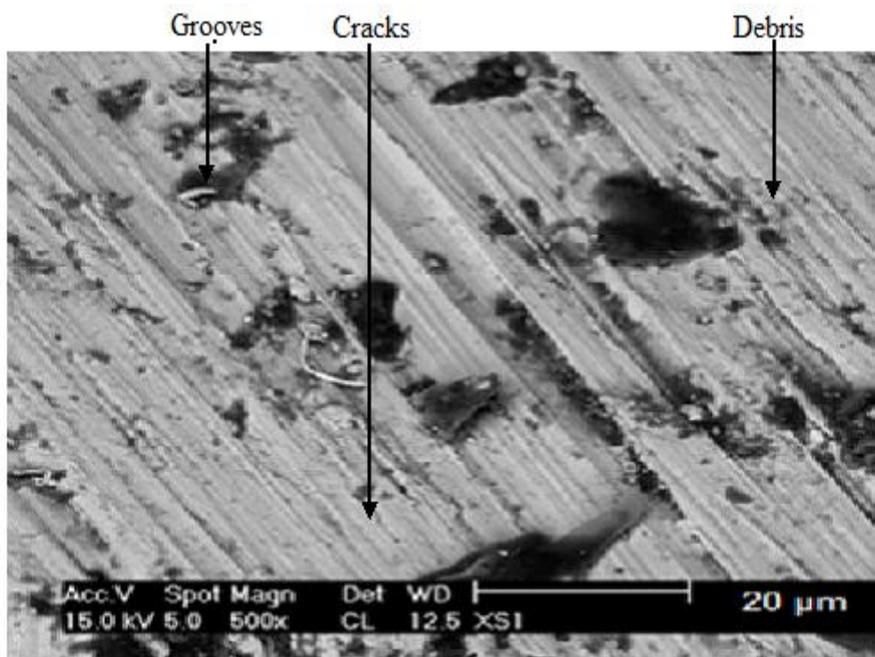**Figure 14.** Variation of the wear mass loss with time

Figure 15. SEM spectrum of the wear scar on the as-received sample

Zn 1 and Zn 2 show little degree of pit formation on the surfaces of the samples but not as much as the mild steel. In the case of Zn 3, (Figure 18) deformation was not visible. This may be due to cohesion of zinc film to the metal surface as a result of applied voltage and eventually justifies the effect of deposition and adhesion mechanism on abrasive wear.
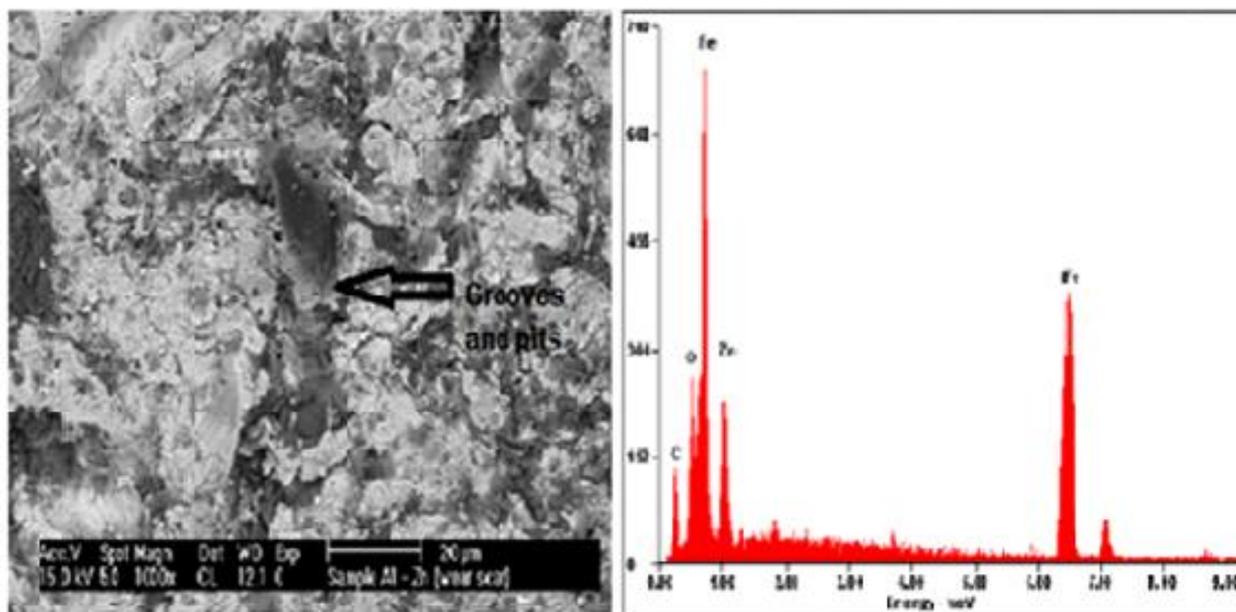

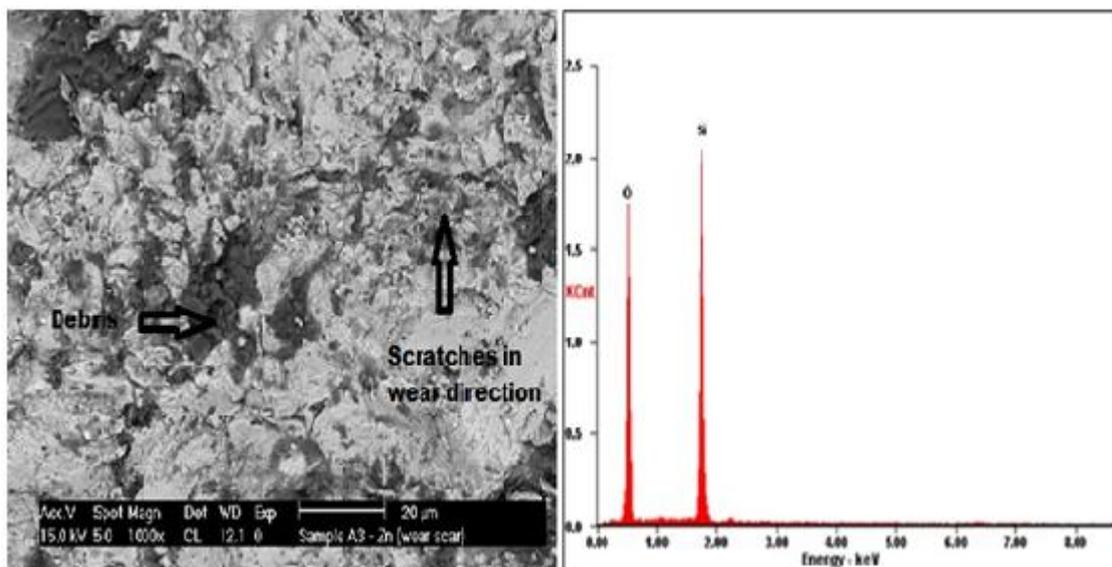**Figure 16.** SEM/EDS spectra of the wear scar on Zn 1

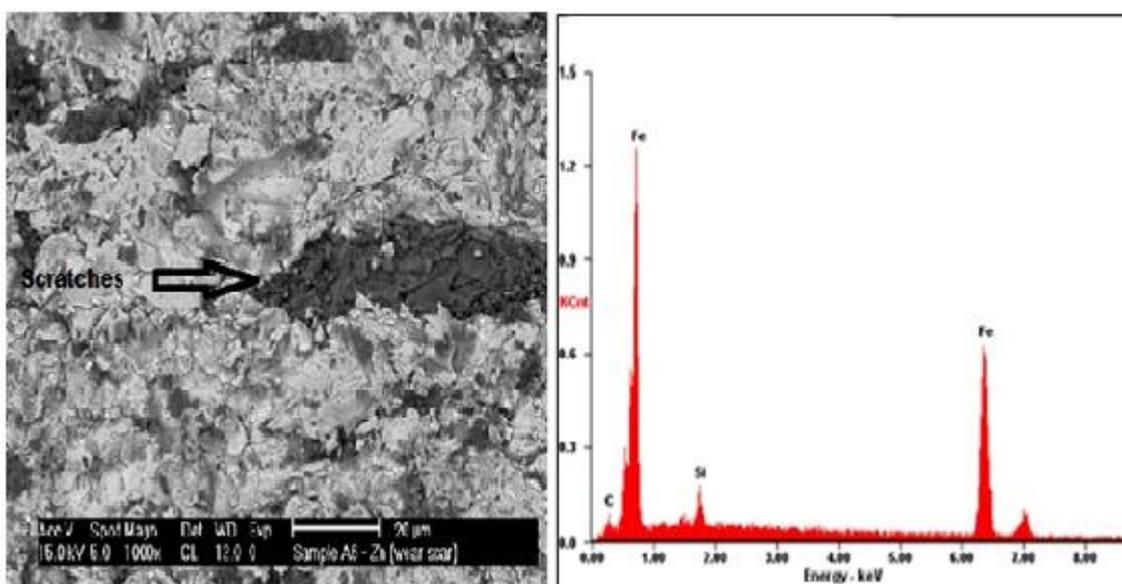**Figure 17.** SEM/EDS spectra of the wear scar on Zn 2

Figure 18. SEM/EDS spectra of the wear scar on Zn 3

3.4. Electrochemical Result

The vulnerability of the deposited samples to corrode in the 3.65% NaCl environment with time was carried out using OCP measurements. The differences in the OCP values of the samples were considered at zero applied current instantly after the dipping of the deposited sample in the different media for one hour. The potential was observed to shift towards less negative values for all the zinc plated samples, with Zn 3 (tending toward more positive) at -0.5 V. This improvement in potential values is due to the effects of Zn electrodeposition. However, the substrate have less passive film

formed on its surface resulting into intensive corrosion attack from the chloride solution with potential value of about -1.5 V which is over double those of the deposited samples.

Table 3. Summary of the potentiodynamic polarization results

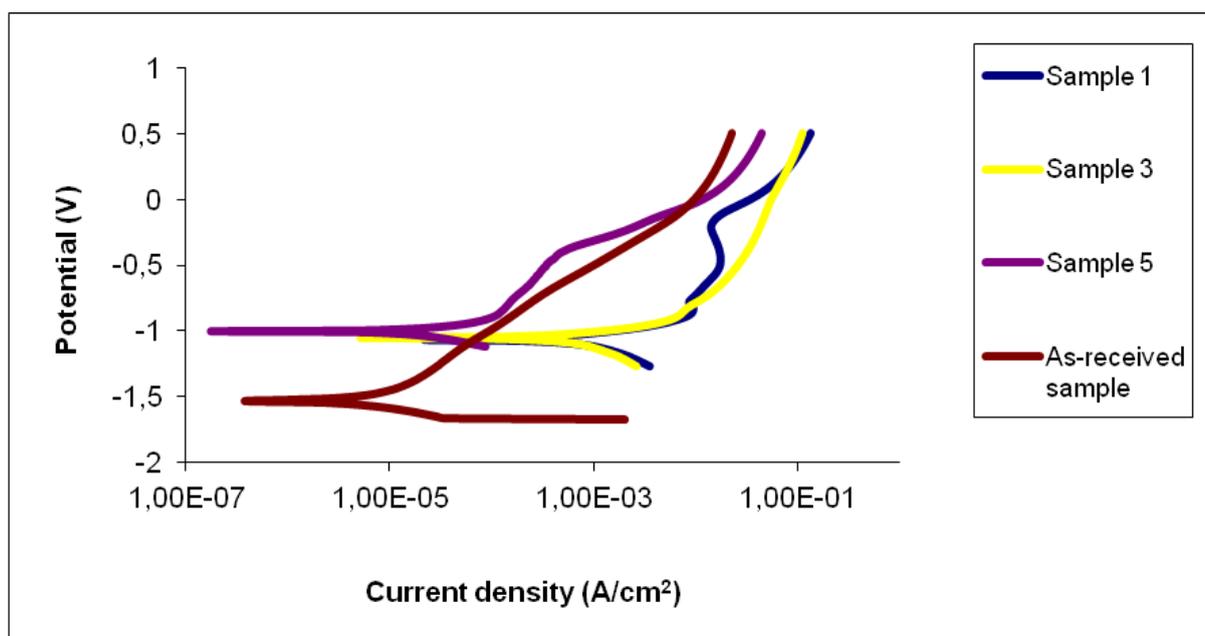| Sample	icorr (A)	Icorr (A/cm2)	RP (Ω)	Ecorr (V)	Corrosion rate (mm/yr)
As-received	2.04×10^{-3}	7.04×10^{-2}	2.76×10^{2}	-1.536	41
Zn 1	1.89×10^{-4}	1.15×10^{-3}	2.97×10^{2}	-1.068	6.7×10^{-1}
Zn 2	6.73×10^{-5}	4.10×10^{-4}	3.15×10^{2}	-1.025	7.4×10^{-2}
Zn 3	2.71×10^{-6}	1.77×10^{-5}	4.56×10^{2}	-1.004	6.6×10^{-2}

Figure 19. Potentiodynamic polarization curves for Zn deposited mild steel

The corrosion performance of the plated Zn 1 to Zn 2 was low and never expected, showing gradual deformation of the protective films. However, Zn 3 was observed to display the highest potential values which confirmed the reason why it exhibited the lowest corrosion rate and highest corrosion resistance in the chloride solution during the potentiodynamic polarization test. The result of polarization measurements for the specimens investigated are summarized in Table 3 and Figure 20.

The mild steel sample had a corrosion current i_{corr} of 2.04×10^{-3} A and a high corrosion rate of about 41 mm/yr due to lack of surface protection. This was attributed to the high anodic potential reached by the sample, absorption of the halide ion on the oxide film which took place at the oxide solution interface and the formation of basic oxide. Meanwhile, Zn 3 showed i_{corr} of 2.71×10^{-6} A; a good decrease in corrosion current which may be due to the formation of very thin ZnO film, which retarded the ingress of chloride ions fully into the plated region and down to the substrate. But, it is good to know that mild steel displayed highest corrosion current density (7.04×10^{-2} A cm^{-2}) than all

deposited samples, while Zn 3 has I_{corr} of 1.77×10^{-5} A cm^{-2}, a three order magnitude decrease in corrosion current density was attained due to the effects of electrodeposition on the substrate. From the polarization resistance (R_p) result, Zn 3 had 4.56×10^{2} (Ω), obviously it was the highest attained for all the coated samples. The order of corrosion resistance is sample 3>2>1. Distinctive surface morphologies of the mild steel and zinc deposited samples after the polarization test are displayed in Figures 21, 22 and 23.
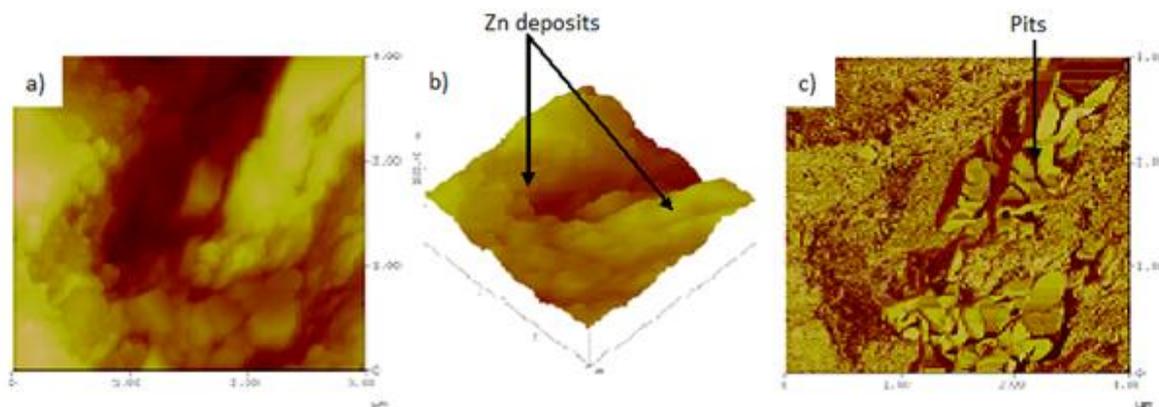

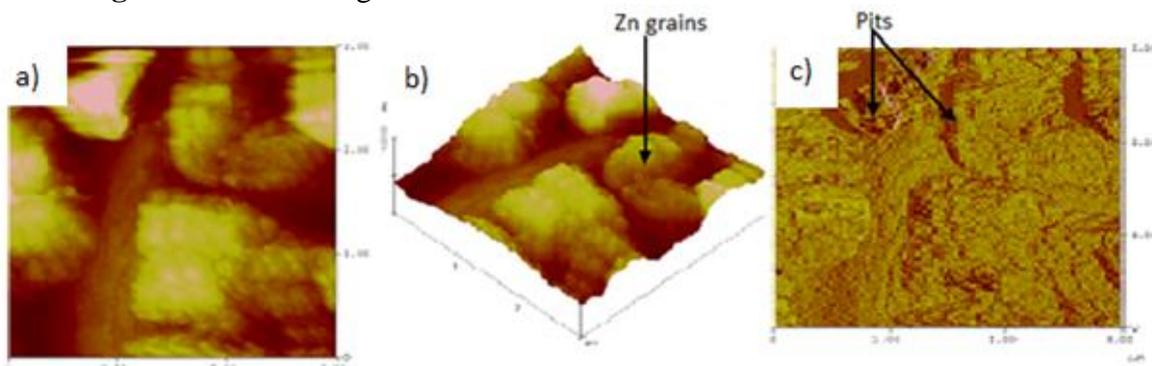**Figure 21.** AFM images of the surface film obtained for Zn 1 after corrosion

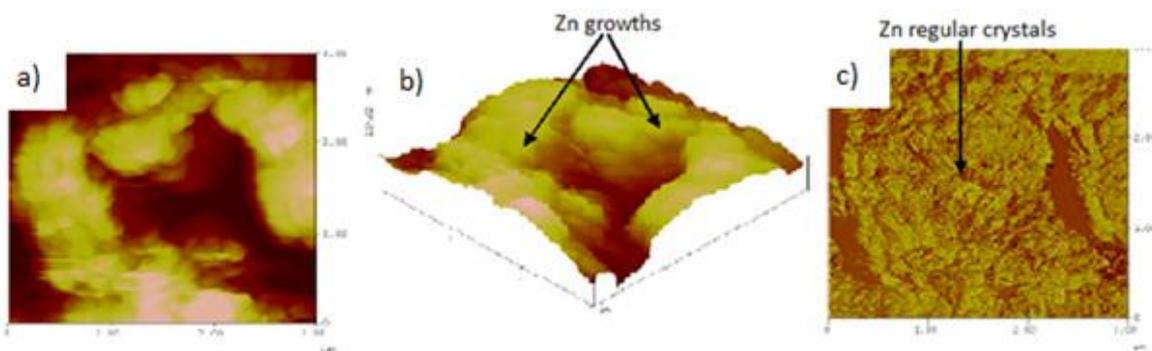**Figure 22.** AFM images of the surface film obtained for Zn 2 after corrosion

Figure 23. AFM images of the surface film obtained for Zn 3 after corrosion

To affirm the stability of the Zn deposited sample after corrosion, Atomic Force Microscope analysis was carried out. Figures 21, 22 and 23 show the AFM of Zn 1, and Zn 2. Obviously Zn 1 and Zn 2 suffered from mild corrosion attack as seen from Figures 21 and 22; the situation greatly improved for Zn 3. The sample (Zn 3) was found to exhibit corrosion potential above other zinc deposited samples. This could be due to the fact that oxide films were totally homogenous and co-deposition stable [19].

From electrochemical principles, the sample with lower corrosion current has lower corrosion rate in the active corrosion stage will exhibit the highest corrosion Zn 3 had the lowest corrosion current as well as lowest corrosion rate hence it has the highest resistance to corrosion.

4. CONCLUSION

Proper electrodeposition of mild steel using zinc particle was carried out. The microhardness and corrosion behaviour of the resultant deposition were investigated with the following deductions:

✓   The average increase in microhardness of the mild steel substrate was 55 HVN to deposited sample Zn 3 was 108 HVN, about twice the microhardness value of the mild steel was achieved.

✓   The corrosion resistance of mild steel was improved after zinc deposition. The sample produced with the highest applied voltage displayed the best microhardness value, and had the highest corrosion resistance. This was featured by a decrease in corrosion current density and corrosion current, increase corrosion potential and the polarization resistance.

✓   The pitting corrosion attack suffered by Zn 1 is attributed to fewer ionic migrations, meaning that only few hydrated ion(s) in the electrolyte migrated toward the cathode under the influence of the applied voltage.

✓   The order of corrosion resistance is sample 3>2>1.

References

1. T.B., Singh, M.N., Singh, D.K. Basu, & S.K. Narang. *J. of Met. and Mat. Sci*. 45, (2003) 199.
2. A.N., Yanjerappa, V.V. Thimmappa, and V.N. Perdur. *Turkish J. of Chem.* 26, (2002) 723.
3. V., Thangaraj, N. Eliaz, and A.Chitharanjan, *J. of Appl. Electrochem*. 39: (2009) 339.
4. T.B. Singh, M.N. Singh, D.K. Basu, and S.K. Narang, *J. of Met. and Mat Sci,* 45, (2003)199.
5. S. Shivakumara, U. Manohar, Y. Arthoba Naik, & T. U. Venkatesha,. *Bull. Mat. Sci*. 30 (2007)
6. C.N. Panagopoules, And M.G.Tsoutsouvaa, *Corr. Eng. Sci. and Tech*., 46, (2011) 513.

7. G.A.G., Pedroza, C.A.C, Souza, I.A. Carlos, and L.R.P. Andrade Lima. *Surface & Coatings Technology,* 206, (2012), 2927.
8. C., Mohankumar, K., Praveen, V., Venkatesha, K. Vathsala, and O. Nayana, *J. of Coat. Tech. Res.,* 9 (1), (2012) 71.
9. C. Mou, Sen X.Sen, And Y.Ming, *J. of Sol. Sta. Electrochem.* 14, (2010) 2235.
10. S. Basavanna, and Y. Arthoba Naik, *J. of Appl. Electroche*m., 39 (2009) 1975
11. I.U. Hague, N. Ahmad, and A. Akhan, *J. of Che. Soc. Pakistani*, 27, (2005) 337.
12. A.P.I Popoola and O.S. Fayomi *Int. J. of Electrochem. Sci*., 6, (2011)3254
13. M.J. Rahman, S.R. Sen, M. Moniruzzaman, and K.M. Shorowordi, *J. of Mech. Eng, Tran*., 40, (2009) 9.
14. A.A. Volinsky, J. Vella, I.S. Adhihetty, V.L. Sarihan, L. Mercado, B.H. Yeung, and W.W. Gerberich, *Mat. Res. Soc*., 649, (2001)1.
15. A.P.I Popoola and O.S. Fayomi, *Sci Res. and Ess*., 6, (2011) 4264-4272.
16. O.S. Fayomi, V.R. Tau, A.P.I. Popoola, B.M. Durodola, O.O. Ajayi, C.A. Loto, and O.A. Inegbenebor,. *J. of Mat. and Env. Sci.*, 3, (2011) 271.
17. A.P.I. Popoola, S.L. Pityana, and O.M. Popoola, *J. of the South Afri. Inst. of Min and Met.,* 111, (2011) 335.
18. A.P.I. Popoola, S.L. Pityana, and O.M. Popoola. *J. of the South Afri. Inst. of Min and Met*., 111 (2011) 345.
19. Princeton Applied Research. Electrochemical Division, 1-8.`
20. A.P.I. Popoola, O.S. Fayomi and O.M. Popoola., O.M. 2011. *Proc. of Mat. Sci. & Tech. Conf., Ohio: Usa*. (2011) 393-400.
21. B. Bobić, S. Mitrović, M. Babić, and I. Bobić, *Tribology in Industry*, 32(1) (2010) 3-11.
22. A.N. Ehteram and H. A. Aisha *Int. J. of Electrochem. Sci*., 3, (2008) 806.